# Modeling and Analysis of Spray Pyrolysis Deposited $SnO_2$ Films for Gas Sensors

**Lado Filipovic, Siegfried Selberherr, Giorgio C. Mutinati, Elise Brunet, Stephan Steinhauer, Anton Köck, Jordi Teva, Jochen Kraft, Jörg Siegert, Franz Schrank, Christian Gspan and Werner Grogger**

**Abstract** Metal oxide materials such as tin oxide ($SnO_2$) show powerful gas sensing capabilities. Recently, the deposition of a thin tin oxide film at the backend of a CMOS processing sequence has enabled the manufacture of modern gas sensors. Among several potential deposition methods for $SnO_2$, spray pyrolysis deposition has proven itself to be relatively easy to use and cost effective while providing excellent surface coverage on step structures and etched holes. A model for spray pyrolysis deposition using a pressure atomizer is presented and implemented in a Level Set framework. A simulation of tin oxide deposition is performed on a typical gas sensor geometry and the resulting structure is imported into a finite element tool in order to analyze the electrical characteristics and thermo-mechanical stress present in the grown layer after processing. The deposition is performed at 400 °C and the subsequent cooling to room temperatures causes a stress to develop at the material interfaces due to variations in the coefficient of thermal expansion between the different materials.

L. Filipovic (✉) · S. Selberherr
Institute for Microelectronics, Technische Universität Wien, Gußhausstraße 27–29/E360, A–1040 Wien, Austria
e-mail: filipovic@iue.tuwien.ac.at

S. Selberherr
e-mail: selberherr@iue.tuwien.ac.at

G. C. Mutinati · E. Brunet · S. Steinhauer · A. Köck
Molecular Diagnostics, Health and Environment, AIT GmbH, Donau-City-Straße 1, A–1220 Wien, Austria
e-mail: Giorgio.Mutinati@ait.ac.at

E. Brunet
e-mail: Elise.Brunet.fl@ait.ac.at

S. Steinhauer
e-mail: Stephan.Steinhauer.fl@ait.ac.at

A. Köck
e-mail: Anton.Koeck@ait.ac.at

G.-C. Yang et al. (eds.), *Transactions on Engineering Technologies*,
DOI: 10.1007/978-94-017-8832-8_22,

**Keywords** Electrical characterization of tin oxide · FEM simulation · Level set method · Modeling spray pyrolysis · Monte Carlo · Smart gas sensors · Spray pyrolysis deposition · Thermal stress modeling · Tin oxide · Von Mises stress

## 1 Introduction

The ability to detect harmful and toxic gases in the environment is a subject of extensive research. Usually, the manufacture of gas sensors is incompatible with that of the CMOS process sequence. The miniaturization of electronic devices has proven to be essential, while bulky gas sensors are still lagging behind the overall progress of CMOS and MEMS devices. Metal oxides may serve as a gas sensing layer, when a thin film of the deposited material is exposed to high temperatures (250–400 °C). A material which has been proven to exhibit all the properties required for good gas sensing performance is tin oxide ($SnO_2$) [5, 20, 24], while others such as zinc oxide (ZnO), indium tin oxide (ITO), CdO, $ZnSnO_4$, NiO, etc. have also been widely studied [4]. This work mainly concerns itself with tin oxide gas sensors and the ability to develop a model which depicts the growth of thin tin oxide layers to act as a gas sensing surface. In addition, the resistance and stress generation through the device after the processing sequence is determined using finite element simulations. The deposition of $SnO_2$ has been reported to be performed using various standard techniques such as chemical vapor deposition [32], sputtering [3], pulsed-laser deposition [30], sol-gel process [6], and spray pyrolysis (SP) deposition [24].

J. Teva · J. Kraft · J. Siegert · F. Schrank
ams AG, Tobelbaderstraße 30, A–8141 Unterpremstätten, Austria
e-mail: Jordi.Teva@ams.com

J. Kraft
e-mail: Jochen.Kraft@ams.com

J. Siegert
e-mail: Joerg.Siegert@ams.com

F. Schrank
e-mail: Franz.Schrank@ams.com

C. Gspan · W. Grogger
Institute for Electron Microscopy and Fine Structure Research, Graz University of Technology and the Centre for Electron Microscopy Graz, Steyrergasse 17, A–8010 Graz, Austria
e-mail: christian.gspan@felmi-zfe.at

W. Grogger
e-mail: werner.grogger@felmi-zfe.at

The spray pyrolysis deposition technique is gaining traction in the scientific community due to its cost effectiveness and relative ease of integration at the back end of a standard CMOS process. The technique is used to grow crystal powders [19], which can then be further annealed for use in gas sensors, solar cells, and other applications. The technique is cost-effective as it involves relatively inexpensive equipment and raw materials and is simple to perform. For these reasons the spray pyrolysis deposition of $SnO_2$ thin films is further explored. A model for spray pyrolysis deposition, which can be incorporated onto a sensor device after a standard CMOS process simulator is desired [11].

Spray pyrolysis requires no vacuum and provides high flexibility in terms of material composition. In order to optimize this technology for the heterogeneous integration of gas sensing layers with CMOS fabricated micro-hotplate chips [15], a complete understanding of the spray pyrolysis deposition process by modeling is a challenging issue. It was our goal to develop and incorporate a model for the growth of ultrathin $SnO_2$ layers into a traditional CMOS process simulator using the Level Set framework [8]. Due to the temperature required for this process (400 °C), the subsequent cooling to room temperature can cause the arise of stress through the device due to the varying coefficients of thermal expansion (CTE) for the different materials. This is explored with finite element simulations.

## *1.1 Smart Gas Sensor Devices*

Different variants of metal oxide based gas sensors, which rely on changes of electrical conductance due to the interaction with the surrounding gas, have been developed. However, today's gas sensors are bulky devices, which are primarily dedicated to industrial applications. Since they are not integrated in CMOS technology, they cannot fulfill the requirements for smart gas sensor applications in consumer electronics. A powerful strategy to improve sensor performance is the implementation of very thin nanocrystalline films, which have a high surface to volume ratio and thus a strong interaction with the surrounding gases. $SnO_2$ has been one of the most prominent sensing materials and a variety of gas sensor devices based on $SnO_2$ thin films has been realized so far [13, 31] as depicted in Fig. 1. The growth of the ultrathin $SnO_2$ layers on semiconductor structures requires a deposition step which can be integrated after the traditional CMOS process [12, 20]. This alleviates the main concern with today's gas sensor devices and their bulky nature, namely high power consumption. The sensing mechanism of $SnO_2$ is related to the chemisorption of gas species over the surface, leading to charge transfer between the gas and surface molecules and changes in the electrical conductance.

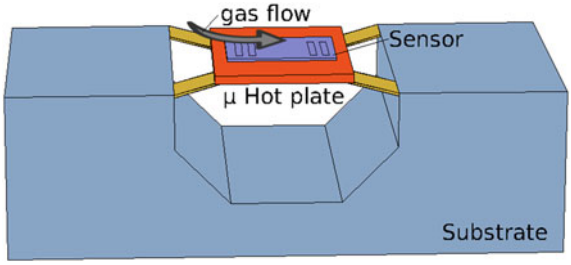


**Fig. 1** Principle view of the gas sensor on a micro hot plate

## *1.2 Level Set Method*

Since the introduction of the Level Set Method by Osher and Sethian [23], it has developed into a favorite technique for tracking moving interfaces. The presented simulations and models function fully within the process simulator presented in [7]. The software also supports memory parallelization during execution [9]. The Level Set method is utilized in order to describe the top surface of a semiconductor wafer as well as the interfaces between different materials. The method describes a movable surface $S(t)$ as the zero Level Set of a continuous function $\Phi(\mathbf{x}, t)$ defined on the entire simulation domain,

$$S(t) = \{\mathbf{x} : \Phi(\mathbf{x}, t) = 0\}. \tag{1}$$

The continuous function $\Phi(\mathbf{x}, t)$ is obtained using a signed distance transform

$$\Phi(\mathbf{x}, t = 0) := \begin{cases} -\min\limits_{\mathbf{x}' \in S(t=0)} \|\mathbf{x} - \mathbf{x}'\| & \text{if } \mathbf{x} \in M(t = 0) \\ +\min\limits_{\mathbf{x}' \in S(t=0)} \|\mathbf{x} - \mathbf{x}'\| & \text{else,} \end{cases} \tag{2}$$

where $M$ is the material described by the Level Set surface $\Phi(\mathbf{x}, t = 0)$. The implicitly defined surface $S(t)$ describes a surface evolution, driven by a scalar velocity $V(\mathbf{x})$, using the Level Set equation

$$\frac{\partial \Phi}{\partial t} + V(\mathbf{x}) \|\nabla \Phi\| = 0. \tag{3}$$

In order to find the location of the evolved surface, the velocity field $V(\mathbf{x})$, which is a calculated scalar value, must be found. For the case of spray pyrolysis deposition, this scalar value is derived using Monte Carlo techniques and ray tracing.

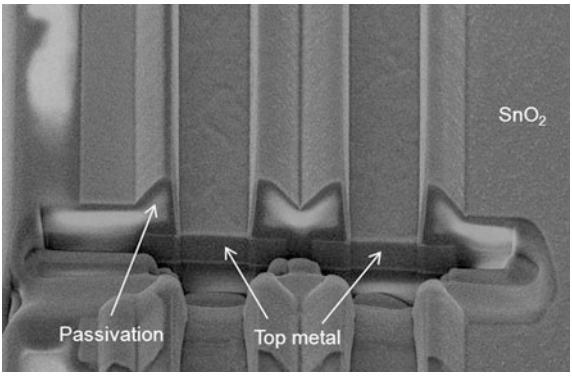


**Fig. 2** Three-dimensional view of the electrode locations on the substrate

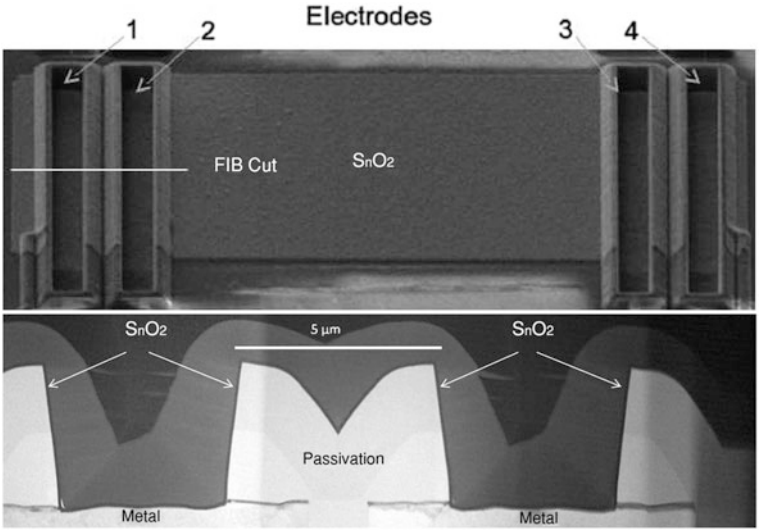


**Fig. 3** View of the electrode locations on the substrate and the side view through the *FIB cut* line

## 2 Tin Oxide Based Gas Sensor

A smart gas sensor device has been manufactured using a 50 nm $SnO_2$ thin film as the sensing material. The device has four electrodes, shown in Figs. 2 and 3, which are stationed above a heat source. The substrate is a CMOS chip with four contact electrodes which are coated with $SnO_2$, as depicted in Fig. 3.

The sensor has been tested in a $H_2$ environment at concentrations down to 10 ppm and the results are depicted in Fig. 4. The sensor itself operates on top of a micro-sized hot plate [29] which heats the sensor locally to 250–400 °C in order to

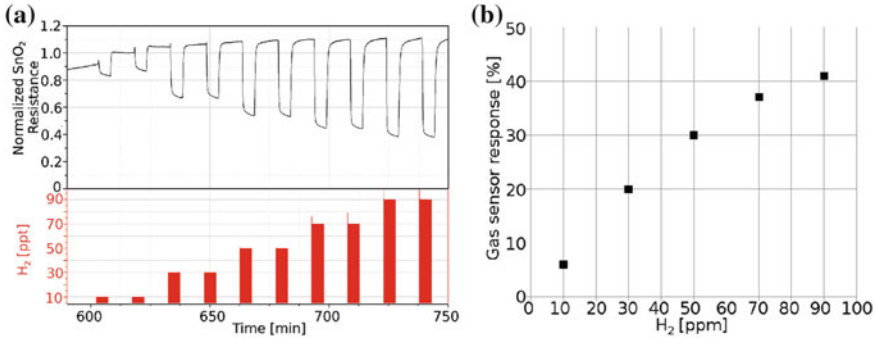


**Fig. 4** **a** $SnO_2$ electrical resistance change. **b** Gas sensor response (%) as $H_2$ in varying concentration is pulsed into a humid synthetic air (RH = 40 %) environment. The sensing temperature is set to 350 °C

detect humidity and harmful gases in the environment, such as CO, $CH_4$, $H_2$, $CO_2$, $SO_2$, and $H_2$ [5].

The gas measurements are performed in an automatic setup to test the functionality of the described $SnO_2$ structure, while heated up to 350 °C. The electrical resistance change is monitored, while pulses of $H_2$ at different concentrations (10–90 ppm) are injected in the gas chamber. Humid synthetic air (RH = 40 %) is used as the background gas. In Fig. 4a, the normalized resistance of the $SnO_2$ structure is plotted for various $H_2$ gas concentrations. In Fig. 4b the gas response, defined as the relative resistance difference in percentage, is shown. The gas sensor results appear to be functional in the entire $H_2$ concentration range investigated.

## 3 Spray Pyrolysis Deposition

During the last several decades, coating technologies have garnered considerable attention, mainly due to their functional advantages over bulk materials, processing flexibility, and cost considerations [21]. Thin film coatings can be deposited using physical methods or chemical methods. The chemical methods can be split according to a gas phase deposition or a liquid phase deposition. Spray pyrolysis is a technique which uses a liquid source for thin film coating. The main advantages of spray pyrolysis over other similar deposition techniques are:

- Cost effectiveness.
- Possible integration after a standard CMOS process.
- Substrates with complex geometries can be coated.
- Uniform process, which can be scaled over larger areas.
- CMOS-compatible temperatures (<400 °C) can be used for processing.

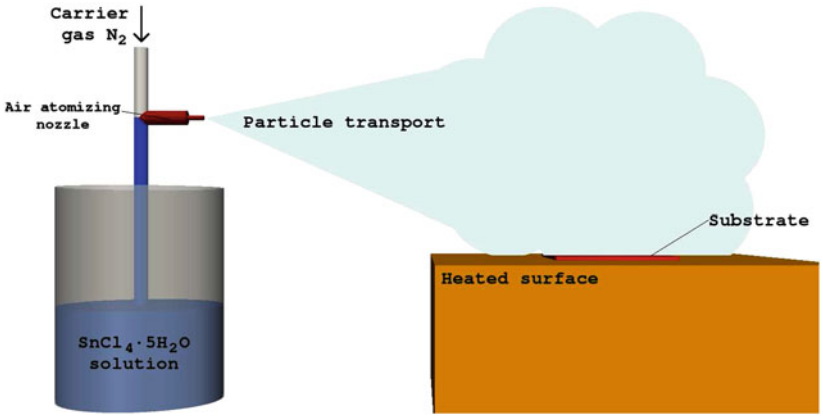


**Fig. 5** Schematic of the spray-pyrolysis deposition process, as set up for $SnO_2$ deposition

Spray pyrolysis is increasingly being used for various commercial processes, such as the deposition of a transparent layer on glass [18], the deposition of a $SnO_2$ layer for gas sensor applications [17], the deposition of a YSZ layer for solar cell applications [25], anodes for lithium-ion batteries [22], and optoelectronic devices [2]. The setup, shown in Fig. 5 is simple and inexpensive when compared to other deposition alternatives.

The three steps which describe the processes taking place during spray pyrolysis deposition are summarized by:

1. Atomization of the precursor solution.
2. Aerosol transport of the droplet.
3. Decomposition of the precursor to initiate film growth.

## *3.1 Experimental Setup*

When depositing a thin film using spray pyrolysis, an ultrasonic, electrical, or gas pressure atomizing nozzle can be used [26]. For smart gas sensor applications, a gas pressure nozzle is ideal due to its ease of use and its ability to create very small droplets which deposit evenly on a desired surface. The retardant forces experienced by droplets during their transport include the Stokes force and the thermophoretic force, while gravity is the only accelerating force, when a gas pressure nozzle is used. An electrical force is included in models which depict ultrasonic or electrical atomizing nozzles [10]. Figure 5 shows a simplified schematic for spraying a specific precursor solution onto the substrate, which is placed on top of a hotplate.

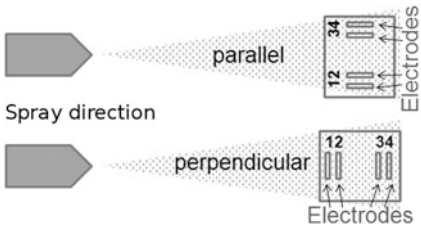


**Fig. 6** Spray direction during deposition

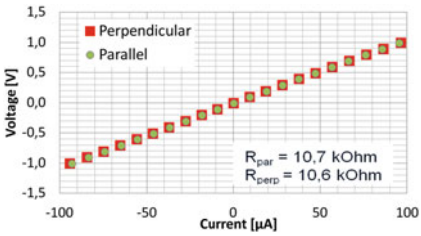


**Fig. 7** V-I curves between electrode 1 and electrode 4 for the chips depicted in Fig. 6

The atomizer has also been adjusted so that the droplets exiting the nozzle are relatively small in volume with an average diameter of approximately 5–10 μm. This ensures that a majority of the droplets reaching the heated wafer surface will evaporate prior to impact, allowing for a uniform deposition of the vapor, which results in a subsequent uniform film growth. In order to ensure that the initial direction of the solution, as it exits the atomizer, does not affect the deposition process, two spray directions have been tested, as shown in Fig. 6.

## *3.2 Experimental Observations*

After performing spray pyrolysis deposition, while directing the spray in parallel and perpendicular to the electrodes, the V-I curves of the two chips are visualized in Fig. 7. It was noted that regardless of the initial spray direction and the direction of the droplets as they leave the atomizing nozzle, the thickness of the grown thin film and its electrical properties remain unchanged.

This is likely due to the nozzle being placed at a distance of approximately 30 cm away from the substrate surface, giving enough time for the Stokes retardant force to effectively remove any influence of the droplets' initial horizontal velocity. Therefore, directionality plays no role in the film deposition process. This also helps to eliminate the potential of large droplets splashing onto the substrate surface. Large droplets generally do not deposit uniformly on the desired surface, but rather impact the heated wafer while in liquid form, leaving behind a powder residue with weak sticking properties to the silicon.

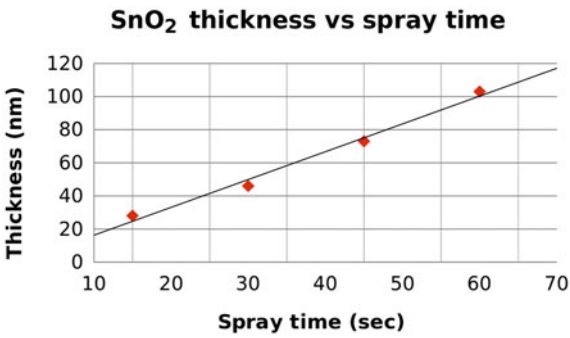


**Fig. 8** The influence of spray time on $SnO_2$ thickness, with temperature set to 400 °C

The thickness of the tin oxide layer depends on the spray temperature and the spray time. With the heatpad temperature set to 400 °C, the thickness of the $SnO_2$ layer is plotted against the spray time in Fig. 8. A linear relationship is evident. The thickness of the grown film does not change, when the deposition takes place on a step structure, as shown in Fig. 9a, suggesting that the deposition is a result of a vapor interaction and not a process which alludes to a direct interaction between the deposition surface and the liquid droplets. Figure 9a shows a resulting $SnO_2$ thin film after a spray pyrolysis deposition step lasting 30 s with the substrate heated to 400 °C. The resulting film thickness is approximately 50 nm. We conclude that the droplets, which carry the depositing material, interact with the substrate surface as a vapor and then deposit in a process analogous to CVD.

## 4 Modeling Spray Pyrolysis

There are two main approaches to modeling spray pyrolysis. One deals with tracking of the trajectories of individual droplets, resulting in their direct impact with the wafer. The second model assumes that the droplets vaporize prior to impact resulting in a CVD-like uniform deposition step.

### *4.1 Modeling the Uniform Deposition Process*

The experimental data shows a linear dependence on spray time and a logarithmic dependence on wafer temperature for the growth rate of the deposited $SnO_2$ layer. A good agreement is given by the Arrhenius expression

$$d_{SnO_2}(t,T) = A_1 t e^{(-E/k_B T)}, \tag{4}$$

where the thickness is given in µm, $A_1 = 3.1\,\mu m/s$, $t$ is the time in seconds, $T$ is the temperature in Kelvin, and $E$ is 0.427 eV.

### 4.2 Spray Pyrolysis as a Vapor Deposition Process

The growth model given in (4) relates the thickness of the deposited material to the applied time and temperature. However, this representation is only valid, when no complex geometries such as deep wells are present. In order to model deposition on a deep well structure, a simulation which considers more than a single deposition rate is required. Since the droplets fully evaporate prior to depositing on the surface, a non-linear simulation model analogous to CVD is used. The implementation requires the combination of the Monte Carlo method within the Level Set framework. A single particle species is considered during deposition. As the simulation is initiated, multiple particles are generated in the simulation space with an average direction perpendicular to and moving towards the wafer. The particles are represented in terms of individual fluxes, given by

$$\Gamma_{src} = \Gamma_{src}(\mathbf{x}; \mathbf{w}, E) \quad \mathbf{x} \in P, \tag{4}$$

where $P$ is the surface which divides the region above the wafer (reactor-scale) and the region comprising the wafer (feature-scale). The flux of particles $\Gamma_{src}$ is described in terms of particles which are moving in direction $\mathbf{w}$ arriving with an energy $E$ per unit area. This energy $E$ depends on the time and temperature of the simulation space, as it is the deciding factor in the speed of the film growth. The distribution of particles stems from the idea that their transport is characterized by the mean free path of a gas $\bar{\lambda}$, which for our process is in the range of 9 mm. In this range, the particle velocities follow the Maxwell-Boltzmann distribution and the flux has a cosine-like directional dependence

$$\Gamma_{src}(\mathbf{x}; q, \mathbf{w}, E) = F_{src} \frac{1}{\pi} \cos\theta \quad \cos\theta = \mathbf{w} \cdot \mathbf{n}_P, \tag{6}$$

where $F_{src}$ is uniform, $\mathbf{n}_p$ is the normal vector to $P$ pointing towards the wafer surface.

In the feature-scale region particles may also be reflected from the wafer walls, modeled with a sticking coefficient, resulting in their deposition elsewhere on the wafer or them leaving the simulation space entirely. Reflected particles follow the Knudsen cosine law [14]. The total flux is then composed of source particles with flux $\Gamma_{src}$ and re-emitted particles, which stick on recursive impact $\Gamma_{re}$. For the spray pyrolysis deposition process, it was found that a sticking coefficient of 0.01 has the best fit to experimental data and was therefore used for the model. The motion of reflected or re-emitted particles is then tracked with their sticking probability reduced after each surface impact. The tracking of a single particle is deemed concluded, when its sticking probability reaches 0.1 % of the original sticking coefficient.

Using the presented model, a simulation was performed for 30 s at 400 °C with the result shown in Fig. 9b. The deposited film has an evenly distributed thickness of approximately 50 nm, as expected from the measured thickness in Fig. 9a. The model is also applied to half of the complete sensor geometry, including two electrodes, as shown in Fig. 3, with the result shown in Fig. 10.

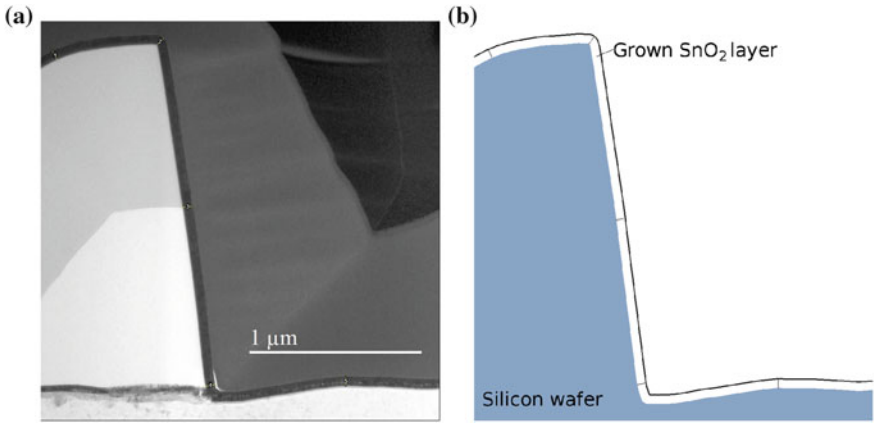


**Fig. 9** Experimental and simulated $SnO_2$ deposition on a step structure. **a** TEM image of a FIB cut. **b** Simulation of **a**

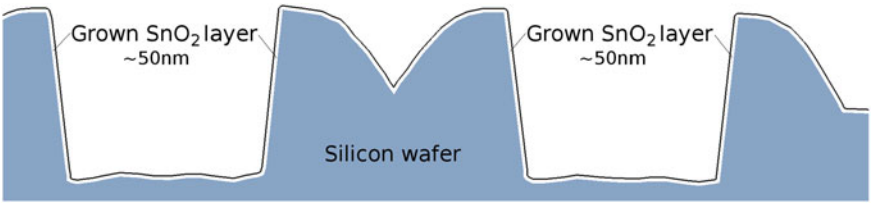


**Fig. 10** The simulation of $SnO_2$ deposition, performed with the heated substrate at a temperature T = 400 °C for a time t = 30 s

## *4.3 Sample Trench Simulations*

With the presented model one can simulate the resulting coverage of various geometries, required for gas sensor manufacturing. For devices which need a large surface area in order to function adequately, it may be more affordable to deposit a layer on trench and well geometries rather than utilizing expensive chip surface area. Therefore, several analysis are performed to estimate at which trench width to depth ratio and at which sidewall angle is the process no longer appropriate. First, we investigate the trench sidewall angle of 5.7° in Fig. 11 and note that for a trench of height 1,000 nm, the separation between the walls must be at least 150 nm in order for no void to form. However, a separation greater than 200 nm is desired in order to ensure no void is formed even when potential variation is introduced in the process.

Similarly, an analysis is performed for a structure with the same dimensions, but with the sidewall angles more vertical at 2°. It was observed that, even at a trench width of 150 nm, a void has formed. Therefore, although vertical walls

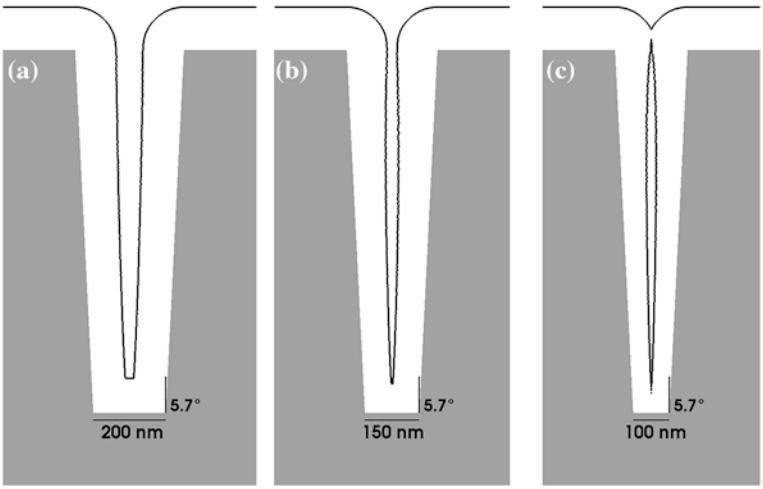


**Fig. 11** Sample $SnO_2$ simulation showing a 60 s spray pyrolysis deposition at 400 °C with a trench depth of 1,000 nm and width ranging between **a** 200 nm **b** 150 nm, and **c** 100 nm. Sidewall angles are set to 5.7°

provide more surface area for the tin oxide to deposit, one must be careful in ensuring enough separation is provided at the top of the trench, where the deposited material tends to accumulate.

In addition, the implemented model can inherently be used to analyze three-dimensional surface coverage, fully integrated in a standard CMOS simulator using a combination of Monte Carlo methods within a Level Set framework.

## 5 Electrical and Stress Analysis of the Sensor Structure

The resulting simulated structure is imported into a finite element tool in order to determine the resistivity and stress distribution in the structure after the processing step. The half-structure is shown in Fig. 12 and the material parameters used are listed in Table 1.

### *5.1 Electrical Resistivity of the Tin Oxide*

The I-V curve for the sensor was experimentally measured in Fig. 7, resulting in a full sensor resistance of 10.7 kΩ. The resistivity of the deposited material is determined using finite element methods. A total resistance of 5.35 kΩ is assumed for the half-sensor structure, which corresponds to a tin oxide resistivity of

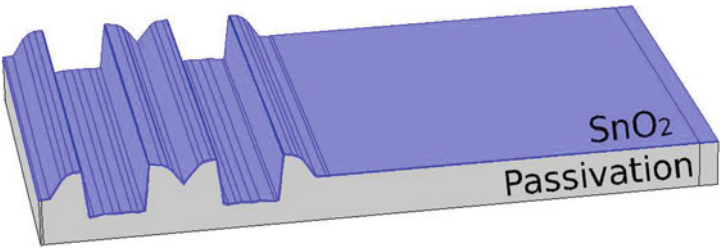


**Fig. 12** The three-dimensional half-sensor structure showing the deposited $SnO_2$ layer, which is imported into the finite element tool for electrical and stress analysis

**Table 1** Electrical and thermal properties of tin oxide

| $SnO_2$ parameter | Value | Units | References |
|---|---|---|---|
| Density | 6.95 | $g.cm^{-3}$ | [1] |
| Electrical resistivity | $1.233 \times 10^{-2}$ | Ω cm | This study, [16, 28] |
| Thermal conductivity | 0.4 | $W{\cdot}cm^{-1}{\cdot}K^{-1}$ | [27] |
| Coefficient of thermal expansion | $4 \times 10^{-6}$ | $K^{-1}$ | [1] |

$1.233 \times 10^{-2}$ Ω cm. This value corresponds to the general range of published values in [16] and [28] for tin oxide. The sensor, when operating at a current of 2 μA [5], experiences a voltage drop of 21.4 mV.

## 5.2 Thermo-Mechanical Stress

After spray pyrolysis deposition and annealing is performed at 400 °C, the structure is cooled to room temperature. This temperature difference can cause stresses between the passivation and the tin oxide material due to their different coefficients of thermal expansion. This stress can lead to material cracking and delamination when the tin oxide does not stick to the passivation layer properly. The stress is determined using the von Mises stress ($\sigma_{VMS}$) as a benchmark, which is defined using a combination of the three principal stresses as

$$\sigma_{VMS} = \sqrt{\frac{1}{2} \cdot (\sigma_1 - \sigma_2)^2 + (\sigma_2 - \sigma_3)^2 + (\sigma_3 - \sigma_1)^2} \tag{7}$$

The tin oxide layer experiences a maximum stress of approximately 1GPa and an average stress of 210 MPa. The interface between the tin oxide layer and the passivation layer experiences a maximum stress of 440 MPa and an average of 120 MPa. The stress distribution in the device is shown with two-dimensional slices through the material in Fig. 13. During the gas sensor operation, the device is frequently heated to temperatures ranging from 200 to 400 °C using the micro

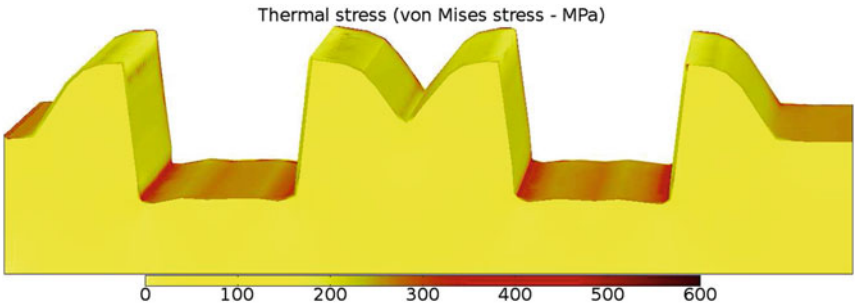


**Fig. 13** The von Mises stress distribution through the passivation and $SnO_2$ layers after processing at 400 °C and cooling to room temperature

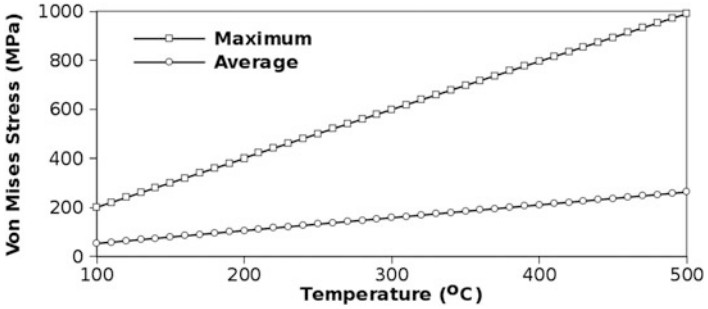


**Fig. 14** The dependence of the maximum and average von Mises stress (MPa) in the $SnO_2$ layer as a result of temperature variation in the sensor

hotplate shown in Fig. 1. This thermal cycling results in further stresses in the tin oxide layer. The effects on the maximum and average stress in the $SnO_2$ layer when cycling the temperature is depicted in Fig. 14. A linear relationship is noted between the applied temperature and generated stress $\sigma_{VMS}$.

## 6 Conclusion

While the general trend for CMOS and MEMS devices has been aggressive miniaturization, gas sensors still generally remain bulky devices the manufacturing of which is difficult to integrate with CMOS processing. The capability of thin metal oxides to detect harmful gases in the environment has lead to the development of smart gas sensors. These oxides can be deposited at the back end of the CMOS process using the spray pyrolysis technique. In this work a model for spray pyrolysis deposition, when an air atomizer is used, has been developed and implemented in a Level Set framework. The model is based on the observation that the material is deposited in a vapor form, analogous to CVD. The deposition of tin

oxide on one half of a typical sensor structure has been simulated and the resulting geometry has been extracted and imported into a finite element tool. The properties of the grown tin oxide has been further analyzed, including the material resistivity and the stress developed in the region as a consequence of the processing step. The deposition is performed at 400 °C and the subsequent cooling to room temperature causes stress development between different layers due to the varying coefficients of thermal expansion between the $SnO_2$ and surrounding passivation.

**Acknowledgements** This work has been partly performed in the COCOA-CATRENE European project and in the project ESiP. In this latter the Austrian partners are funded by the Austrian Research Promotion Agency (FFG) under project no. 824954 and the ENIAC Joint Undertaking.

## References

1. M. Batzill, U. Diebold, The surface and materials science of tin oxide. Prog. Surf. Sci. **79**(2), 47–154 (2005)
2. G. Blandenet, M. Court, Y. Lagarde, Thin layers deposited by the pyrosol process. Thin Solid Films **77**(1–3), 81–90 (1981)
3. J. Boltz, D. Koehl, M. Wuttig, Low temperature sputter deposition of $SnO_x$: Sb films for transparent conducting oxide applications. Surf. Coat. Technol. **205**(7), 2455–2460 (2010)
4. A. Bouaoud, A. Rmili, F. Ouachtari, A. Louardi, T. Chtouki, B. Elidrissi, H. Erguig, Transparent conducting properties of Ni doped zinc oxide thin films prepared by a facile spray pyrolysis technique using perfume atomizer. Mater. Chem. Phys. **137**(3), 843–847 (2013)
5. E. Brunet, T. Maier, G.C. Mutinati, S. Steinhauer, A. Köck, C. Gspan, W. Grogger, Comparison of the gas sensing performance of $SnO_2$ thin film and $SnO_2$ nanowire sensors. Sens. Actuator B **165**, 110–118 (2012)
6. D.M. Carvalho, J.L. Maciel Jr, L.P. Ravaro, R.E. Garcia, V.G. Ferreira, L.V. Scalvi, Numerical simulation of the liquid phase in $SnO_2$ thin film deposition by sol-gel-dip-coating. J. Sol-Gel. Sci. Technol. **55**(3), 385–393 (2010)
7. O. Ertl, Numerical methods for topography simulation. Dissertation, Technischen Universität Wien, Fakultät für Elektrotechnik und Informationstechnik, http://www.iue.tuwien.ac.at/phd/ertl/ (2010)
8. O. Ertl, S. Selberherr, A fast level set framework for large three-dimensional topography simulations. Comput. Phys. Commun. **180**(8), 1242–1250 (2009)
9. L. Filipovic, O. Ertl, S. Selberherr, Parallelization strategy for hierarchical run length encoded data structures. In *Proceedings of IASTED International Conference on Parallel and Distributed Computing and Networks (PDCN) 2011*, 15–17 Feb 2011, Innsbruck, Austria, pp. 131–138 (2011)
10. L. Filipovic, S. Selberherr, G.C. Mutinati, E. Brunet, S. Steinhauer, A. Köck, J. Teva, J. Kraft, J. Siegert, F. Schrank, Modeling spray pyrolysis deposition. In *Lecture Notes in Engineering and Computer Science: Proceedings of World Congress on Engineering 2013*, 3–5 July 2013, London, UK, pp. 987–992 (2013)
11. L. Filipovic, S. Selberherr, G.C. Mutinati, E. Brunet, S. Steinhauer, A. Köck, J. Teva, J. Kraft, J. Siegert, F. Schrank, C. Gspan, W. Grogger, Modeling the growth of thin $SnO_2$ films using spray pyrolysis deposition. In *Proceedings of International Conference on Simulation of Processes and Devices (SISPAD) 2013*, 3–5 Sept 2013, Glasgow, UK, pp. 208–211
12. L. Filipovic, S. Selberherr, G.C. Mutinati, E. Brunet, S. Steinhauer, A. Köck, J. Teva, J. Kraft, J. Siegert, F. Schrank, A method for simulating spray pyrolysis deposition in the level set framework. Eng. Lett. **21**(4), 224–240 (2013)

13. W. Göpel, K. Schierbaum, $SnO_2$ sensors: current status and future prospects. Sens. Actuator B **26**(1–3), 1–12 (1995)
14. J. Greenwood, The correct and incorrect generation of a cosine distribution of scattered particles for Monte-Carlo modelling of vacuum systems. Vacuum **67**(2), 217–222 (2002)
15. C. Griessler, E. Brunet, T. Maier, S. Steinhauer, A. Köck, J. Teva, F. Schrank, M. Schrems, Tin oxide nanosensors for highly sensitive toxic gas detection and their 3D system integration. Microelectron. Eng. **88**(8), 1779–1781 (2011)
16. J. Joseph, V. Mathew, J. Mathew, K. Abraham, Studies on physical properties and carrier conversion of $SnO_2$:Nd thin films. Turkish J. Phys. **33**, 37–47 (2009)
17. G. Korotcenkov, V. Brinzari, J. Schwank, M. DiBattista, A. Vasiliev, Peculiarities of $SnO_2$ thin film deposition by spray pyrolysis for gas sensor application. Sens. Actuator B **77**(1–2), 244–252 (2001)
18. S. Major, A. Banerjee, K. Chopra, Highly transparent and conducting indium-doped zinc oxide films by spray pyrolysis. Thin Solid Films **108**(3), 333–340 (1983)
19. G.L. Messing, S.C. Zhang, G.V. Jayanthi, Ceramic powder synthesis by spray pyrolysis. J. Am. Ceram. Soc. **76**(11), 2707–2726 (1993)
20. G. Mutinati, E. Brunet, S. Steinhauer, A. Köck, J. Teva, J. Kraft, J. Siegert, F. Schrank, E. Bertagnolli, CMOS-integrable ultrathin $SnO_2$ layer for smart gas sensor devices. Procedia Eng. **47**, 490–493 (2012)
21. A. Nakaruk, C. Sorrell, Conceptual model for spray pyrolysis mechanism: fabrication and annealing of titania thin films. J. Coat. Technol. Res. **7**(5), 665–676 (2010)
22. S.H. Ng, J. Wang, D. Wexler, S.Y. Chew, H.K. Liu, Amorphous carbon-coated silicon nanocomposites: a low-temperature synthesis via spray pyrolysis and their application as high-capacity anodes for lithium-ion batteries. J. Phys. Chem. C **111**(29), 11131–11138 (2007)
23. S. Osher, J.A. Sethian, Fronts propagating with curvature-dependent speed: algorithms based on Hamilton-Jacobi formulations. J. Comput. Phys. **79**(1), 12–49 (1988)
24. G. Patil, D. Kajale, V. Gaikwad, G. Jain, Spray pyrolysis deposition of nanostructured tin oxide thin films. ISRN Technol. **2012**(1–5), 275872 (2012)
25. D. Perednis, L.J. Gauckler, Solid oxide fuel cells with electrolytes prepared via spray pyrolysis. Solid State Ion. **166**(3–4), 229–239 (2004)
26. D. Perednis, L.J. Gauckler, Thin film deposition using spray pyrolysis. J. Electroceram. **14**(2), 103–111 (2005)
27. C. Poulier, D. Smith, J. Absi, Thermal conductivity of pressed powder compacts: tin oxide and alumina. J. Eur. Ceram. Soc. **27**(2), 475–478 (2007)
28. K. Shamala, L. Murthy, K.N. Rao, Studies on tin oxide films prepared by electron beam evaporation and spray pyrolysis methods. Bull. Mater. Sci. **27**(3), 295–301 (2004)
29. M. Siegele, C. Gamauf, A. Nemecek, G.C. Mutinati, S. Steinhauer, A. Kock, J. Kraft, J. Siezert, F. Schrank, Optimized integrated micro-hotplates in CMOS technology. In *Proceedings of IEEE International New Circuit and Systems Conference (NEWCAS) 2013*, 16–19 June 2013, Paris, France, pp. 1–4 (2013)
30. S. Sinha, R. Bhattacharya, S. Ray, I. Manna, Influence of deposition temperature on structure and morphology of nanostructured $SnO_2$ films synthesized by pulsed laser deposition. Mater. Lett. **65**(2), 146–149 (2011)
31. A. Tischner, T. Maier, C. Stepper, A. Köck, Ultrathin $SnO_2$ gas sensors fabricated by spray pyrolysis for the detection of humidity and carbon monoxide. Sens. Actuators B **134**(2), 796–802 (2008)
32. I. Volintiru, A. de Graaf, J. Van Deelen, P. Poodt, The influence of methanol addition during the film growth of $SnO_2$ by atmospheric pressure chemical vapor deposition. Thin Solid Films **519**(19), 6258–6263 (2011)